# MODELLING A TURBOGENERATOR FOR WASTE HEAT RECOVERY ON A DIESEL-ELECTRIC HYBRID BUS

**Ian Briggs**

*School of Mechanical & Aerospace Engineering*,
*Queen's University Belfast, Northern Ireland.*
*BT9 5AH*

**Abstract**

An increase in global oil consumption, coupled with a peak in oil production has seen the price of fuel escalate in recent years, and consequently the transport sector has been forced to take measures to reduce fuel consumption in vehicles. In addition, ever-tightening legislation is forcing automotive manufacturers to invest in technology to reduce toxic emissions.

In response to these issues, this project aims to address one of the fundamental issues with the Internal Combustion Engine — approximately one third of the fuel energy supplied to the engine is lost as heat through the exhaust system. By recovering some of this wasted heat energy on a diesel-electric hybrid bus, the fuel consumption can be significantly reduced.

This report details how turbocompounding can be applied to a small-capacity diesel engine, via the inclusion of a turbogenerator, and assesses its waste heat recovery performance. With this aim in mind, a brief state of the art of turbogenerating is presented, and an evaluation of its suitability for a hybrid bus application is outlined.

The development and validation of a one-dimensional engine model using *WAVE* is discussed, to which a turbogenerator is then included. The effects on fuel consumption are investigated and the results show it is possible to configure the model so as to improve brake specific fuel consumption by approximately 1.2%, and total system power may be increased by up to 7.55% by recovering waste exhaust energy.

# 1 Introduction

Recent decades have seen a huge increase in global demand for energy, driven by population growth and industrial development. Worldwide energy consumption is projected to increase by up to 36% by 2035, driven by a population which is predicted to grow by 25% in the same period [1].

Since the Industrial Revolution, dependence on fossil fuels has been cemented. The number of vehicles on the road is constantly increasing, while the more recent affordability of air travel has also contributed to a surge in fuel usage.

The International Energy Agency predicts a massive increase in demand for oil in non-OECD countries such as India and China as shown in Figure 1, with the transportation sector in these countries playing a pivotal role in driving the demand for fossil fuels. Their rapidly expanding population, coupled with the desire to own and run more vehicles is likely to see a sharp increase in demand for fuel, above the rate of oil production.

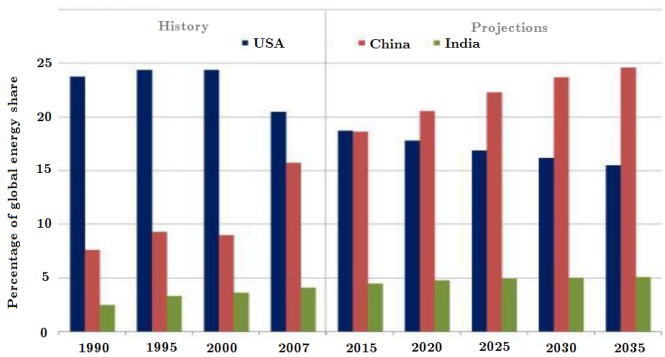


Figure 1: Share of world energy consumption (source: International Energy Agency)

Indeed, it is generally thought that the rate of global oil production is nearing, or already experiencing a peak, after which it will steadily decline. It is likely that, given this increased demand and reduced supply, oil prices will continue to rise above previously seen trends.

The combination of increased prices and a gradual reduction in available oil places an importance on not only finding alternative fuels for human needs, but of improving the efficiency of the ever-increasing number of vehicles which rely on fossil fuels.

There is now a suspected link between emissions of gases and long-term environmental damage, highlighted by a rise in average global temperatures. However, limits on greenhouse gas emissions such as carbon dioxide ($CO_2$) have only recently begun to be implemented by government bodies, usually through tax incentives rather than mandatory limits. Strict controls have, however, been implemented on toxic emissions in many countries and the European Emissions Standards set limits

on the amount of toxic gases such as mono-nitrogen oxides ($NO_x$), carbon monoxide (CO) and hydrocarbons (HC) that are permissible in the exhaust of transport vehicles.

This emissions legislation, coupled with rising fuel costs has made it much more pressing to concentrate on improving the efficiency of road vehicles. This is noted by the number of technologies and studies which aim to do just that. The majority of effort made by vehicle manufacturers has focused on mechanical drivetrain elements or aspects of combustion which have large effects on fuel consumption. Some of these methods are listed below:

- Light-weight materials [2], [3];
- Homogeneous Charge Compression Ignition (HCCI) [4]-[6];
- Variable Valve Timing (VVT) [7], [8];
- Turbocharging [9];
- Dual-clutch gearbox [10], [11].

These technologies are described in detail elsewhere but while they can successfully reduce fuel consumption, primarily through modifying elements of the combustion process or parts of the engine, they do not (with the exception of turbocharging) address the fundamental problem that a considerable amount of fuel energy is still wasted through the exhaust system.

Attempting to capture this wasted energy by converting the heat in the exhaust line into useful power can achieve further reductions in fuel consumption. With approximately 30% of the fuel energy supplied to a turbocharged diesel engine lost through the exhaust as heat, there is significant scope for recovering and making use of this energy.

The method of heat recovery chosen for this project is turbocompounding which consists of a small ‘power’ turbine mounted on the exhaust line of the engine. The power generated by the turbocompound may be fed back to the engine or used to power various auxiliaries on the vehicle; depending on the form of turbocompounding implemented. This is discussed in the next section.

# 2 Turbocompounding

There are three main methods of turbocompounding typically in use. These are:

- Mechanical Turbocompounding;
- Turbogenerator;
- Electric Turbocharging.

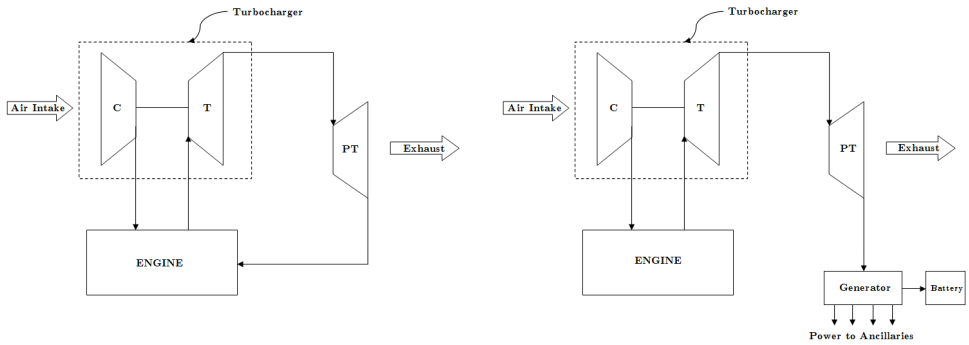


(a) Mechanical turbocompounding (b) Turbogenerator

Figure 2: Turbocompounding schematic layouts

In mechanical turbocompounding and the turbogenerator, wasted hot gases are fed from the turbocharger turbine to a second power turbine as shown in Figure 2.

Mechanical turbocompounding connects the power turbine directly to the engine's crankshaft via a system of gears as in Figure 2(a), while a turbogenerator connects the power turbine to an electric generator (Figure 2(b)) which can be used to directly power the electrical components of the engine via a battery.

The third method of turbocompounding, electric turbocharging, consists of a small generator fitted on the shaft of the turbocharger (Figure 3).

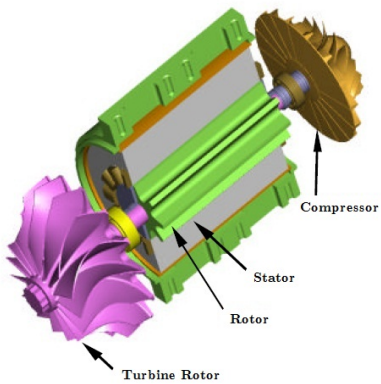


Figure 3: Electric turbocharger (adapted from [16])

While the electric turbocharger is suited to tightly-packaged applications, [12]-[16], the main drawback is that it involves changing the existing turbomachinery. For this project, this would require recertification of the bus, which is a time-consuming and costly procedure. It is therefore not favoured by the manufacturer and as such it will not be investigated further in this project.

Turbogenerating is the preferred method as it has none of the complexities involved with the gear systems in a mechanical turbocompounding setup and allows the power extracted from the generator to be varied or controlled. An example of a turbogenerator is shown in Figure 4 which highlights the compact nature of the device. Results for a heavy-duty diesel engine show a turbogenerator can lead to a 10% improvement in brake specific fuel consumption (BSFC) [17]; significantly better than mechanical turbocompounding, which delivered a 3% improvement.

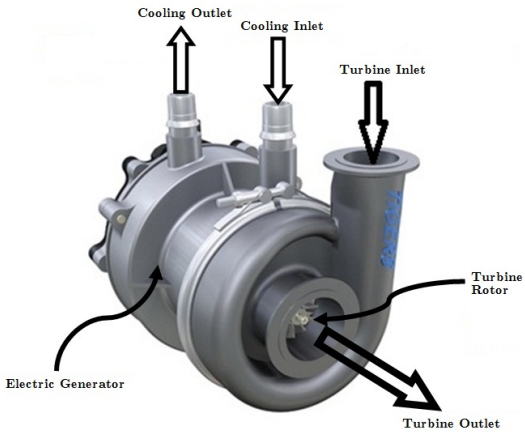


Figure 4: Water-cooled version of *TIGERS* (adapted from: Green Car Congress)

Another benefit of the turbogenerator is its flexible operation. A plot of the turbocompound performance map is shown in Figure 5. The turbocompound map is limited on the left side by the maximum turbine inlet temperature and on the right by the maximum turbocharger speed, while the fuelling ratio curves represent engine power levels.

A mechanical turbocompound is usually limited to a single power line, while the ability to control the turbogenerator independently of engine speed means it can operate anywhere on a power curve between the two limits [16]. This means turbogenerators have the ability to operate nearer to the turbine temperature limit, thereby maximising the engine's fuel efficiency.

In a study of mechanical turbocompounding [18], a standard setup is used, with a power turbine downstream of the turbocharger turbine. The model varies geometric parameters in order to achieve the amount of power required to drive the compressor (i.e. boost pressure) and supply the engine,

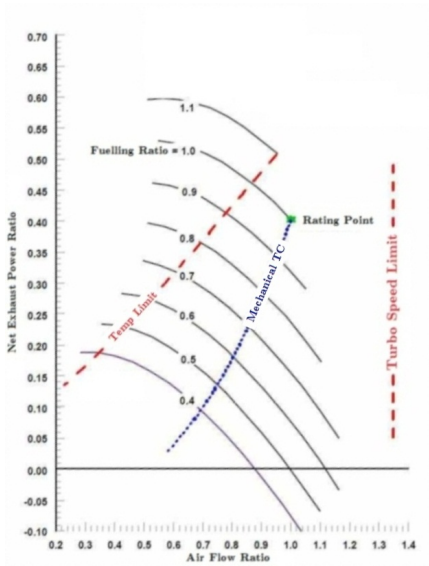


Figure 5: Turbocompound map (adapted from [16])

while the power remaining is used for conversion to electricity, thus giving the total power of the system. The model is calibrated at a single operating point and compared well to experimental data in both engine performance and $NO_x$ emissions. The electric generator efficiency was assumed constant at 95%, typical of switched reluctance motors.

The report outlines a 4.5% reduction in BSFC at full load, reducing to a negligible amount at 25% load. As turbine pressure ratio increases, engine power decreases almost linearly. Net engine power decreases from 352kW to 325kW. However, as power turbine pressure ratio increases, power generated also increases, and if the pressure ratio is maintained in the region 1.7-1.9, the power generated is around 35kW, leading to a 2.3% increase in total system power. The effect on emissions is a reduction of between 12% and 17% in NOx at the optimum power turbine pressure ratio.

It is reported in [19] how engine performance is affected by a turbogenerator during a transient study. Two models are presented: one consists of a turbocharged heavy-duty diesel engine operating on biogas, while the other consists of the same setup with the addition of a turbogenerator.

It is noted that total power throughout the range of engine speeds is higher with the turbogenerated engine than the standard turbocharged engine. However, crank torque is lower when the turbogenerator is added. This is because the turbogenerator is removing some work from the energy of the system, and the presence of the turbogenerator increases the amount of backpressure in the system.

Overall efficiency is also greater with the turbogenerator included. Peak system efficiency rises from 43.5% to almost 46% at an engine speed of approximately 1600rpm. It is shown that efficiency can be increased by varying the turbogenerator speed during the transient. The greater the engine speed, and the greater the turbogenerator speed, the greater the benefit.

Various layouts of turbogenerator are also discussed [20]-[23] where a serial layout is used with a bypass pipe to divert flow around the power turbine (Figure 6(a)). This allows the turbogenerator to avoid creating excessive backpressure, and also serves as a fail-safe mechanism where the flow can be diverted should a fault develop in the generator [22].

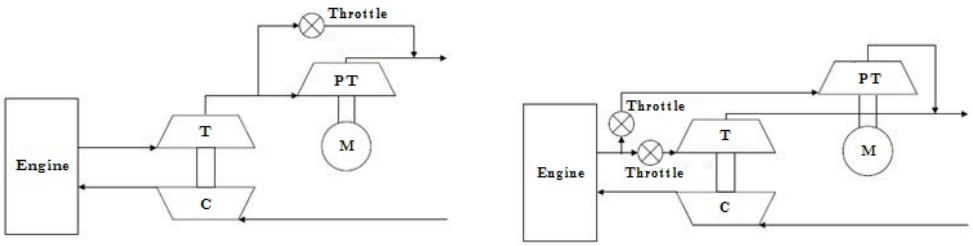


(a) Serial Layout (b) Parallel Layout

Figure 6: Turbogenerator layout options (adapted from [20])

Figure 6(b) also suggests an alternative layout where the power turbine is run in parallel to the turbocharger turbine. This configuration produces the best performance, though the author does not discuss whether this is due to the layout or the differences in turbine rotor designs, volute designs and operating conditions of the power turbine in each configuration.

This literature review has proven that a turbogenerator is the most suitable method of turbocompounding for the hybrid bus application. Its small footprint is ideal for the tightly packaged engine bay of the bus, while the hybrid system available on the bus allows the electrical power generated by the turbogenerator to be easily stored in the existing battery packs.

The performance of the turbogenerator will be assessed by creating a computational model of the engine used on the bus and subsequently installing a turbogenerator in the model to quantify the power generated and the effects on the fuel consumption of a hybrid bus.

# 3 Modelling

## 3.1 Introduction

This phase of the project took the findings from the literature review presented in section 2 and created a computational model of a diesel engine, which was validated against experimental data.

A turbogenerator was then be fitted to the model, and its suitability for the hybrid bus platform was assessed. The methodology for the modelling procedure is as follows:

1. Obtain engine geometry measurements;
2. Create baseline engine model;
3. Install turbogenerator in the model;
4. Optimise system operation;
5. Assess impact on hybrid bus drive cycle.

The first four steps of this solution procedure will be described below, but the final step of the process (assessing the impact on a hybrid bus drive cycle) involves the use of an externally developed model. This external model (hereafter called the 'hybrid bus model') was developed by *QUB* in association with *Wrightbus* and takes an engine performance map and uses data such as road route, gradient, acceleration/deceleration and the use of air conditioning to assess the overall performance of the bus. However, while the hybrid bus model captures a considerable amount of data relating to the profile of the drive cycle, it cannot by itself model components of the engine or the exhaust line, and hence cannot model heat recovery techniques.

This highlights the need for a detailed model of the engine and turbogenerator. The output of this engine model will provide an engine performance map which will form the input for the hybrid bus model.

## 3.2 Engine Modelling

The details of the engine used in the hybrid bus (Figure 7) are:

- Ford Duratorq diesel engine;
- 2.4-litre capacity;
- Turbocharged (with variable geometry turbine)

This engine has been tested extensively by one of the technical partners in the project, *Revolve Ltd.*, and a comprehensive set of test data is available which will be used to both set up and validate the engine model that is created.

The engine modelling will be carried out using *WAVE*[*] engine modelling software. Extensive training in the software package was completed via tutorials and the initial model was created based on one of these tutorial examples before being extensively developed.

[*] *WAVE* engine modelling software provided by *Ricardo Ltd.*

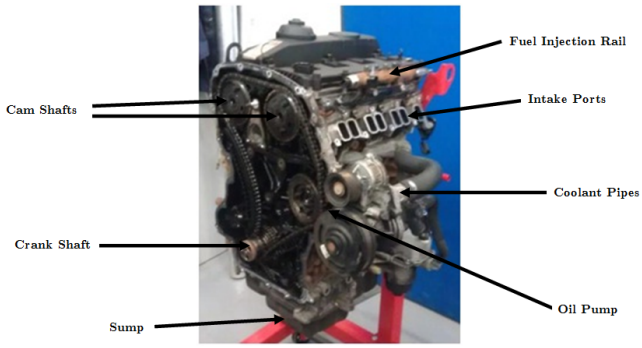


Figure 7: Ford Duratorq 2.4-litre turbocharged diesel engine

*QUB* obtained an example of the engine as shown in Figure 7, and this enables geometric measurements to be obtained in order to create the model. Initial measurements were taken of basic geometric parameters such as intake and exhaust manifold dimensions (Figure 8(a)). These were obtained by measuring pipe lengths, diameters and bend angles using flexible wire and Vernier calipers.

Intake and exhaust port dimensions were obtained using Vinamold; a pourable moulding compound which sets to allow accurate examination of the internal dimensions of the ports (Figure 8(b)). Valve dimensions were measured, and lift profiles were obtained using a gauge (Figure 8(c)), and the values and profiles obtained have been used in the creation of the baseline engine model.

(a) (b) (c)

Figure 8: Measurements procedure for: (a) Intake Manifold, (b) Intake & Exhaust Ports and (c) Valves

Other engine data such as bore, stroke, compression ratio as well as valve timing have been obtained from *Revolve* and did not need to be measured, although con-rod length has been measured, and used in the model. All these parameters are shown in Table 1 and have been used to create the baseline model.

Table 1: Basic Engine Information

| **Parameter** | **Value** |
|---|---|
| No. of Cylinders | 4 |
| Bore | 89.9mm |
| Stroke | 94.6mm |
| Con-rod length | 150.0mm |
| Compression Ratio | 17.5 |
| Displacement | 2402cc |
| Intake Valve Opens | 9.0°BTDC |
| Intake Valve Closes | 37.0°ABDC |
| Exhaust Valve Opens | 49.0°BBDC |
| Exhaust Valve Closes | 9.0°ATDC |

As mentioned previously, the turbine used in the turbocharger of the engine is of a variable geometry-type. However, there are no turbine maps available for this turbine. As a modelling workaround, a fixed geometry turbine may be used with a variable mass flow multiplier applied. This scales the mass flow passing through the turbine and imitates the way a variable geometry turbine works when it alters its stator vane positions.

## 3.3 Model Details

An engine model was created using the geometric data obtained from suppliers and as detailed in § 3.2. The engine model, which is created in schematic form in *WAVE*, is shown in Figure 9.

This schematic representation of the engine layout allows for a clear understanding of its operation. The main components such as engine block, compressor, turbine and turbogenerator power turbine are clear to see. Fuel injectors are connected directly to each cylinder, while the compressor and turbine of the turbocharger are connected via a shaft which is free to rotate. The power turbine of the turbogenerator can be seen downstream of the turbocharger turbine, connected to a shaft.

The pipes of the intake and exhaust manifolds are created from the physical geometries measured from the engine. Bend angles, pipe diameters, pipe lengths are fed into a data panel for each pipe, along with wall thicknesses and material properties which are used to calculate heat transfer. There are also implementations of heat exchangers to model the Charge Air Cooler and the Exhaust Gas Recirculation (EGR) Cooler.

The turbogenerator is represented as a turbine with a generic performance map installed. This map is scaled from the default turbine map present in *WAVE* to represent a turbine rotor smaller of suitable size. The initial model development focused on the validation of a baseline engine model (with the turbogenerator switched off). This was carried out in the model by closing the valve upstream of the power turbine and fully opening the valve on the bypass line (see Figure 9). Doing

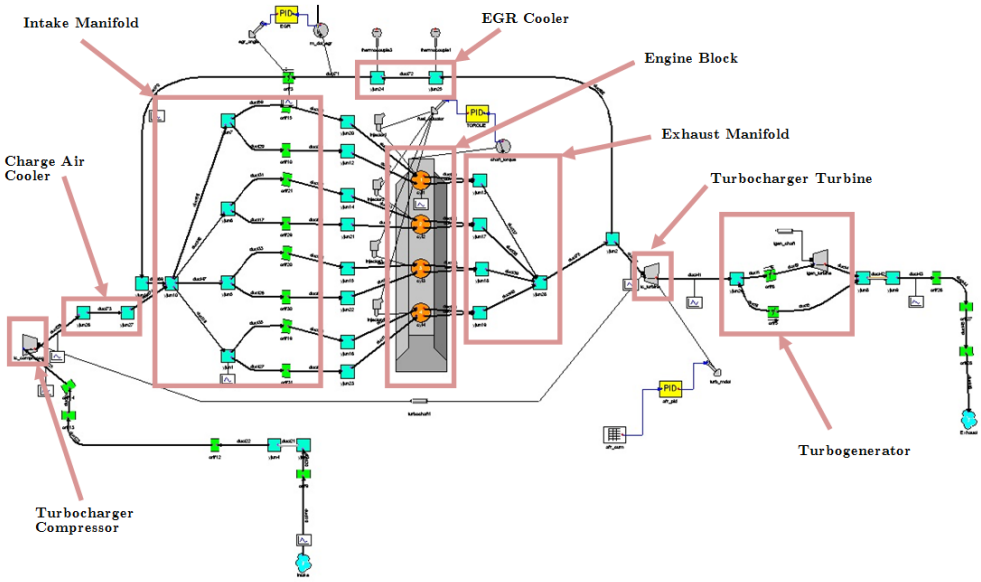


Figure 9: Schematic Layout of Engine Model

so ensures no flow passes through the power turbine and the model is then performing in the same way as the baseline engine on the test bed.

Various PID controllers are present in the model and these are explained further in § 3.4.

## 3.4 Model Control

Various input targets are specified based on values obtained from experimental measurement. The target values used as model inputs are:

- Brake Torque;
- Air to Fuel Ratio (AFR);

The model is then controlled via a series of PID controllers which change various model parameters in order to achieve the target values described above. The PID controllers and their functions are listed below:

- PID1: Targets brake torque by varying fuel rate;
- PID2: Targets AFR by varying turbine mass flow multiplier as described in § 3.2;

- PID3: Targets EGR mass flow rate by varying EGR valve angle.

*WAVE's* inbuilt calibration tool was used to obtain gain values for each controller. This ensured the controllers were properly calibrated to achieve the target values as quickly as possible. Care was taken to ensure this process was completed successfully, to ensure the controllers could work together due to the closely-coupled nature of their control parameters.

### 3.5 Limitations

Various parameters required for the construction of a detailed model are unknown due to a lack of in-cylinder experimental test data. The main area of uncertainty surrounds in-cylinder pressures, burn data and turbocharger maps which would validate the model created in *WAVE*. This means that experience and data from literature must be used for some of the input parameters.

Although compressor performance maps have been obtained and input into the model, the absence of turbine performance maps could lead to errors in predicting boost pressures. But since experimental data is available which states these pressures, it is feasible to adjust the turbocharger maps to achieve the expected levels of boost.

Similarly, no data is available for ignition and combustion data such as burn duration or burn rate. Estimates can be made at all of these parameters which can be verified by examining other results such as air and fuel flow rates and volumetric efficiency, but it must be noted that there is some uncertainty over these aspects of the model until they can be verified by analysing suitable results.

## 4 Results

### 4.1 Baseline Engine Model

As this project is focused on the performance of a hybrid bus, the main parameter of interest is brake specific fuel consumption (BSFC). The results for BSFC for the baseline engine are presented in Figure 10(a). This plot shows how the engine performs in terms of BSFC across its operating range. For each operating speed and load point (represented as torque in this plot) a value of BSFC is shown and, as is typical of diesel engines, the most efficient operating point is towards the upper left corner of this map. It is this data which will be used in future steps to assess the performance of the bus over its drive cycle.

A comparison of how well the model performs compared to experimental data is shown in Figure 10(b). This shows that the overall error between simulation and prediction across the majority of the map is less than 2%. Although this provides a good level of confidence in the model, there are some noticeable errors at low engine speeds where the difference between predicted and measured

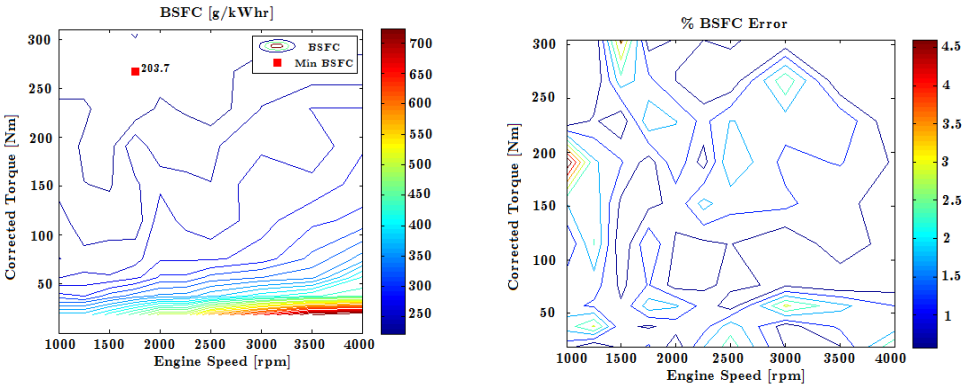


(a) BSFC Prediction (b) BSFC Error

Figure 10: Baseline model BSFC prediction

data is around 4.5%. This still represents good agreement between the simulated and experimental results.

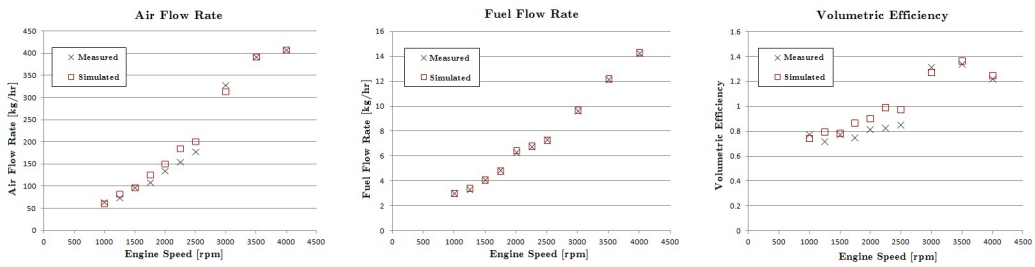


(a) Air Flow (b) Fuel Flow (c) Volumetric Efficiency

Figure 11: Validation results for mid load

Results for air and fuel flow rates and volumetric efficiency at mid-load are shown in Figure 11. The good agreement between measured and predicted data gives confidence in the underlying physical models in *WAVE*. The generally positive match of air flow rate suggests that the engine is breathing in the correct amount of air, which in turn means the intake geometry is modelled correctly and the EGR loop is performing as expected.

Similarly, the agreement in the fuel flow rate, which corresponds directly to the BSFC data, suggests that the burn data used in the model is accurate and the correct amount of fuel is being injected and burned within the cylinder. These predictions are backed up by a similar agreement in volumetric efficiency. In the absence of real validation data, these results give confidence in the combustion model used.

## 4.2 Turbogenerator Model

The previous section detailed the validation of the baseline engine model. The next stage of development is to activate the turbogenerator.

Initial runs of the model with the turbogenerator activated highlighted numerous problems associated with the operation of the system. When the turbogenerator was activated, the amount of flow trying to pass through its turbine was so high at some operating points, that the turbine became choked. This meant the pressure upstream of the turbogenerator turbine (backpressure) became unfeasibly high and this in turn caused the pressure to rise upstream of the turbocharger turbine, and the boost pressure increased. Consequently, a lot of the flow was forced to travel through the open EGR circuit. This combination of high backpressure and open EGR circuit means that the engine could not produce useful power, and the simulation would fail.

This problem arose before the model incorporated a PID controller to regulate Air to Fuel Ratio (AFR), and was caused by the method used to replicate the variable geometry turbine in the model, i.e. allowing the mass flow to scale; to overcome the backpressure the engine had to produce very high boost pressures which in turn caused AFR to rise above that of the baseline model. Consequently, the controller on the turbine was modified to match AFR of the baseline case as described in § 3.4, thus limiting the amount of boost pressure produced. This allows a working model to be achieved.

The turbogenerator model was then run at five significant operating conditions. These points were extracted from an analysis of typical bus drive cycle data which highlighted the most frequently accessed points of the operating map. The results are shown on the BSFC map in Figure 12.

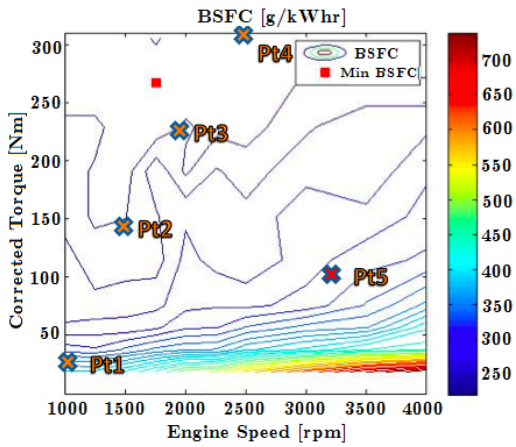


Figure 12: Load points examined in initial turbogenerator model runs

Initially the turbogenerator speed is fixed at 40,000rpm, a representative figure based on litera-

ture, and a summary of the results is shown in Table 2. These results clearly show that the benefits of the turbogenerator configuration are limited to a small area of the operating map (Pt 2) where a small reduction in BSFC is obtained and a moderate increase in power is generated. At all other points, although considerable power is produced in some cases, an *increase* in BSFC is observed.

Table 2: Turbogenerator Model Results: shaft speed set to 40,000rpm

| **Operating Point** | **Change in Total Power** | **Change in BSFC** |
|---|---|---|
| Pt 1 | +0.33% | +1.35% |
| Pt 2 | +3.98% | -0.67% |
| Pt 3 | +0.97% | +0.16% |
| Pt 4 | +1.73% | +1.17% |
| Pt 5 | +2.36% | +2.85% |

However, the shaft speed was subsequently increased to 90,000rpm and the results for this run are shown in Table 3. In this instance, the results are much more encouraging. Four of the five points investigated offer an improvement in BSFC over the baseline case. 'Pt 3' offers the best improvement in fuel consumption (1.2%), and it is encouraging that this is closest to what is already the most efficient area of the map.

Table 3: Turbogenerator Model Results: shaft speed set to 90,000rpm

| **Operating Point** | **Change in Total Power** | **Change in BSFC** |
|---|---|---|
| Pt 1 | +0.52% | +2.67% |
| Pt 2 | +1.66% | -1.02% |
| Pt 3 | +3.23% | -1.20% |
| Pt 4 | +4.62% | -1.04% |
| Pt 5 | +7.55% | -0.59% |

At the other points the reduction in BSFC is slightly less significant; between 0.59% and 1.04%. However, the turbogenerator is still capable of producing significant power at these points (a 4.62% increase at 'Pt 4' and a 7.55% increase at 'Pt 5').

At 'Pt 1' there is an insignificant amount of power produced and a noticeable BSFC penalty at both shaft speeds, and in formulating an operating strategy for the turbogenerator, in practice, the device would be best switched off in this area of the performance map.

Clearly, the difference in power produced, and the change in BSFC, is highly dependent on turbogenerator shaft speed. An energy audit provides a useful tool to analyse the flow of energy through the engine. An example is shown for 'Pt 5' in Figure 13.

The balance of fuel energy can be seen split between various paths, and the majority of fuel energy goes towards brake work; the energy required to create power from the engine. Most of the

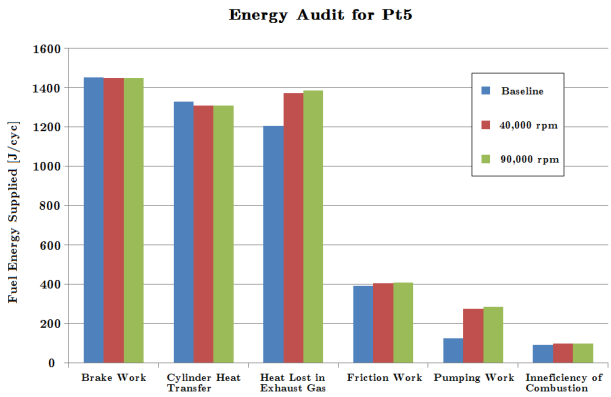


Figure 13: Energy balance for 'Pt 5' with varying turbogenerator shaft speed

other parameters vary by just a small amount when the turbogenerator is activated, but there is a significant increase in both the heat lost in the exhaust gases, due to the presence of the turbogenerator, and increased pumping work when the turbogenerator is applied. The pumping work doubles between the baseline model and the turbogenerator models; indicating that more work is required during the exhaust stroke to overcome the backpressure created by the device itself. However, the pumping work seems largely independent of turbogenerator shaft speed, which suggests that the performance benefit of the 90,000rpm case is largely due to the turbine operating more efficiently at this higher speed.

The turbogenerator has thus far been run at two operating speeds, and variation in this parameter will be studied in more depth as part of an optimisation study later in the project. It is envisaged that this optimisation work will focus on varying the turbogenerator shaft speed and size of the turbogenerator turbine rotor. Currently, the results show that it is possible to operate the turbogenerator in such a way that total system power may be increased by up to 7.55%, and the brake specific fuel consumption may be reduced by 1.20%.

# 5 Conclusions & Recommendations

This project aims to recover some of the heat wasted on a diesel-electric hybrid bus. To achieve this, turbocompounding will be used by installing a second 'power' turbine on the exhaust line.

An extensive literature review has been conducted into various types of turbocompounding and the turbogenerator has been chosen as the most suitable method for this project due to its relative simplicity of operation, its small size and the ease of which the power it generates may be integrated

with the existing hybrid power storage on the bus.

A computational model of the engine currently used in the bus has been created (baseline model) and this has been fully validated against a set of experimental data. This validation showed the error between the simulated brake specific fuel consumption and the measured value to be generally less than 2% across a wide operating range.

This validated baseline model was then extended by including a turbogenerator. This has showed that for one load and speed point, an increase in system power of 3.23% could be generated with a net BSFC saving of approximately 1.20%. The maximum increase in total power produced from the device is 7.55% at full load.

The future development of this work will focus on running the turbogenerator model across the operating range of the engine to see what level of performance may be achieved at other load points. The effects of this performance on the hybrid bus will be quantified via the use of an external model which simulates the drive cycle of the bus. A subsequent period of optimisation will refine the performance of the turbogenerator and its operating strategy over a typical bus drive cycle, looking at parameters such as turbine rotational speed and turbine rotor size.

## Acknowledgement

The author would like to thank Geoff McCullough, Stephen Spence and Roy Douglas at Queen's University Belfast. He would also like to thank the project partners Wrightbus Ltd and Revolve Ltd for supplying validation data, and Cedric Rouaud, Jiri Navratil and Johan Bernards at Ricardo Ltd for technical support with the WAVE software. The work has been funded by Technology Strategy Board and Invest Northern Ireland.

## References

[1] Int. Energy Agency, World Energy Outlook 2010. [Online]. Available: http://www.worldenergyoutlook.org/docs/weo2010/WEO2010_es_english.pdf [Accessed: 2 Jun. 2011].

[2] M. Lapp et al., "Advanced Connecting Rod Design for Mass Optimization", Proc. Soc. Automotive Engineers World Congr. And Exhibition: Reliability and Robust Design in Automotive Engineering, Detroit, USA, 2010, SAE Technical Paper 2010-01-0420.

[3] I. Tanaka, et al., "Engine Weight Reduction Using Alternative Light Materials", Proc. Soc. Automotive Engineers Passenger Car Conf. & Exposition, Dearborn, USA, 1992, SAE Technical Paper 922090.

[4] “MIT researchers work toward spark-free, fuel-efficient engines”, [Online]. Available: http://web.mit.edu/newsoffice/2007/engine-0723.html [Accessed 9 Jun 2011].

[5] K. Epping, et al., “The Potential of HCCI Combustion for High Efficiency and Low Emissions”, Proc. Soc. Automotive Engineers Future Car Congr., Crystal City, USA, 2002, SAE Technical Paper 2002-01-1923.

[6] “Homogeneous Charge Compression Ignition (HCCI) Technology”, [Online]. Available: http://www-erd.llnl.gov/FuelsoftheFuture/pdf_files/hccirtc.pdf [Accessed: 10 Nov. 2011].

[7] “BMW’s Valvetronic”, [Online]. Available: http://autospeed.com/cms/title_BMWs-Valvetronic/A_111539/article.html [Accessed: 16 Jan 2012].

[8] T. Lancefield et al., “The application of variable event valve timing to a modern diesel engine”, Proc. Soc. Automotive Engineers World Congr. And Exhibition: Variable Valve Actuation, Detroit, USA, 2000, SAE Technical Paper 2000-01-1229.

[9] R. K. Turton, Principles of Turbomachinery, 2nd ed. London, UK: Chapman and Hall, 1992.

[10] “Efficient Dual Clutch EDC, Automatic Transmission”, [Online].Available: http://www.renault.com/en/Innovation/gamme-mecanique/Pages/transmission-dct.aspx [Accessed: 25 Mar 2011].

[11] “Volkswagen medium van is first with DCT”, [Online]. Available: http://www.dctfacts.com/in-the-market/volkswagon-medium-van.aspx [Accessed: 25 Mar 2011].

[12] B. Sendyka and J Soczwka, “Recovery Of Exhaust Gases Energy By Means Of Turbocompound”, Proc. 6th Int. Symp. Diagnostics and Modeling of Combustion In Internal Combustion Engines,Yokohama, Japan, 2004, pp. 99-103.

[13] J. Bumby, S. Crossland and J. Carter, “Electrically Assisted Turbochargers: Their Potential For Energy Recovery”, Proc. Hybrid Vehicle Conf., Inst. Eng. and Technology, Coventry, UK, 2006, pp. 43-52.

[14] A. Greszler, “Diesel Turbo-compound Technology”, Presentation to ICCT/NESCCAF Workshop, San Diego, USA, 2008.

[15] U. Hopmann and M. Algrain, “Diesel Engine Electric Turbo Compound Technology” Soc. Automotive Engineers Technical Paper 2003-01-2294, 2003, doi:10.4271/2003-01-2294.

[16] F. Gerke, “Diesel Engine Waste Heat Recovery Utilizing Electric Turbocompound Technology”, Proc. 7th Diesel Engine Emissions Reduction (DEER) Workshop, Portsmouth, USA, 2001.

[17] I. Thompson, “Investigation into the Effects of Turbocompounding”, Differentiation Report, School of Mechanical and Aerospace Engineering, Queen’s University Belfast, Northern Ireland, unpublished, 2009.

[18] D. Hountalas, C. Katsanos and V. Lamaris, “Recovering Energy for the Diesel Engine Exhaust Using Mechanical and Electrical Turbocompounding”, Proc. Soc. Automotive Engineers Int. World Congr., Detroit, USA, 2007. SAE Paper Number 2007-01-1563.

[19] I. Thompson, S. Spence, C. McCartan, D. Thornhill and J. Talbot-Weiss, “Investigations Into the Performance of a Turbogenerated Biogas Engine During Speed Transients” Proc. ASME Turbo Expo, Vancouver, Canada, 2011.

[20] A. M. I. Mamat, A. Romagnoli1 and R. F. Martinez-Botas, “Design and Development of a Low Pressure Turbine For Turbocompounding Applications”, Proc. IGTC 2011, Osaka, Japan, 2011.

[21] M. Michon et al., “Modelling and Testing of a Turbo-generator System for Exhaust Gas Energy Recovery”, Proc. Vehicle Power and Propulsion Conf., Arlington, USA, 2007, pp. 544-550.

[22] M. Michon et al., “Switched Reluctance Turbo-Generator for Exhaust Gas Energy Recovery”, Proc. IEEE Power Electron. Motion Control Conf., Portoroz, Slovenia, 2006, pp. 1801-1807.

[23] W. Wei, W. Zhuge, Y. Zhang and H. Yongsheng, “Comparative Study on Electric Turbo-Compounding Systems for Gasoline Engine Exhaust Energy Recovery”, Proc. ASME Turbo Expo 2010: Power for Land, Sea, and Air (GT2010), Glasgow, UK, 2010, Paper no. GT2010-23204, pp. 531-539.